Polymer Chain Dynamics of Core−Shell Thermosensitive Microgels

J. Rubio Retama,[†,‡] B. Frick,[§] T. Seydel,[§] M. Stamm,[‡] A. Fernandez Barbero,[||] and E. López Cabarcos*[,†]

Department of Pharmaceutical Chemical-Physics, University Complutense of Madrid, 28040 Madrid, Spain, Leibniz-Institut für Polymerforschung Dresden, Hohe Strasse 6, Dresden 01069, Germany, Institut Laue Langevin, Grenoble, France, and Complex Fluid Physics Group, Department of Applied Physics, University of Almería, E-04120 Almería, Spain

Received March 26, 2008; Revised Manuscript Received May 8, 2008

ABSTRACT: Microgels of poly(*N*-isopropylacrylamide) (PNIPAM) have the ability to change size in response to temperature. PNIPAM microgels with 0.25 wt % cross-linker content were used to investigate the molecular dynamics of the polymer chains in the swollen and collapsed states. The study was performed using incoherent elastic (IES) and quasielastic neutron scattering (IQNS), and pulsed field gradient NMR spectroscopy (PFG−NMR). From IES the volume transition is characterized by a sharp increase of the elastic intensity at the transition temperature. Using IQNS, a diffusive motion of the polymer chains was identified with self-diffusion coefficient $D = 1.1 \pm 0.2 \times 10^{-11}$ m^2/s at 290 K which decreases down to $D = 8.6 \pm 0.1 \times 10^{-13}$ m^2/s when the microgel deswells at 327 K. With PFG−NMR spectroscopy we measured two diffusion coefficients in the swollen state that are associated with regions of high and low cross-linking content in the microgel. IQNS and PFG−NMR spectroscopy measurements demonstrate that in the swollen state the polymer is behaving as if it is in solution whereas in the collapsed state it resembles as a solid material.

Introduction

Microgels are cross-linked polymeric networks with a size typical for colloidal particles. When many of those particles form a complex system, features coming from their individual soft nature and from their collective colloidal character become apparent. Since the pioneering work of Pelton et al.,[1] there has been a great interest in the synthesis of smart microgels, which can undergo the volume phase transition by external stimuli such as temperature, pH, ionic strength, or the action of external fields.[2,3] Due to its stimuli responsive property, this sort of materials are promising colloidal systems for cutting edge applications such as drug delivery, chemical separations, etc. Among others PNIPAM microgels are interesting thermosensitive colloidal systems, showing a volume phase transition[4,5] from swollen to collapsed states at around 307 K. This property has prompted increased scientific interest for the potential applications to nano and biotechnology.[6−11]

The mesh structure of PNIPAM microgels was studied using small angle neutron scattering and dynamic light scattering by our team. A heterogeneous core−shell model with most of the cross-linkers placed at the core region was proposed.[12] A body of later literature supports the proposed core−shell model.[13−15] However, dynamical studies in gels and microgels are not so numerous.[16−18] A theory for the dynamics of the gel fiber network in the swollen state together with experimental results in polyacrylamide gels was presented by Tanaka et al.[16] The dynamics of PNIPAM gels in the swollen state has been investigated by dynamic light scattering and it was found that the collective diffusion coefficient increases by increasing the polymer volume fraction and by swelling.[17] More recently, swelling and deswelling kinetics of PNIPAM macrogels with 3 wt % cross-linking content was investigated.[18] However, the influence of the volume transition on the dynamics of the microgel network has not yet been investigated. In this paper, we report on the dynamics of the PNIPAM microgel network in the swollen and the collapsed states using incoherent neutron scattering and pulse field gradient NMR.

Experimental Section

Materials. PNIPAM microgels were prepared by radical polymerization of an emulsifier free aqueous solution of *N*-isopropylacrylamide at 75 °C using and *N*,*N*′-methylene bis(acrylamide) as cross-linker and ammonium persulphate as initiator.[19] Following this method, we obtained spherical microgels with narrow size distribution that present the typical PNIPAM volume phase transition at around 34 °C (see Figure 1). We have selected for our study

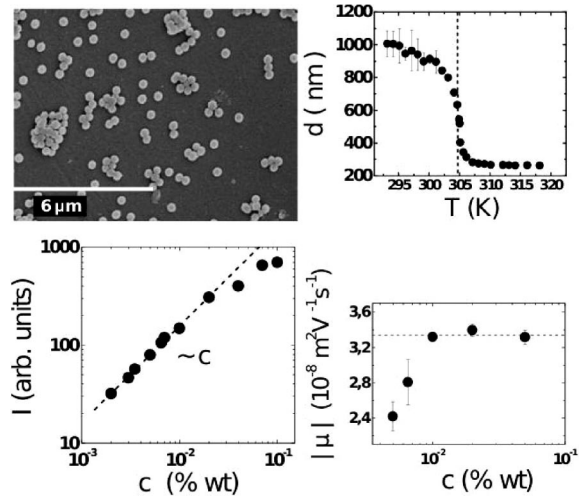

Figure 1. SEM micrograph of dry PNIPAM microgeles (top left). The diameter of the thermosensitive particles against temperature is shown in top right part. The mean light scattering intensity (bottom left) and the electrophoretic mobility (bottom right) of the colloidal particles, from where the concentration range for single scattering and low particle interaction was determined, are shown as function of particle concentration.

* Corrsponding author. E-mail: cabarcos@farm.ucm.es. Telephone: 34-91394 1751. Fax: 34-91394 2032.
[†] Department of Pharmaceutical Chemical-Physics, University Complutense of Madrid.
[‡] Leibniz-Institut für Polymerforschung Dresden.
[§] Institut Laue Langevin.
[||] Complex Fluid Physics Group, Department of Applied Physics, University of Almería.

10.1021/ma800668t CCC: $40.75
Published on Web 06/11/2008

a microgel with 0.25 wt % cross-linking density because it shows a steep volume change in a narrow temperature range.

For neutron scattering and NMR experiments, samples were prepared by dispersing the microgels in D_2O to obtain contrast between the polymer and the solvent. The concentration was kept dilute (3 wt.-%) to diminish colloidal interactions as well as multiple scattering. The technical aspects of the sample preparation had been reported previously.[12]

Methods. The study of the molecular dynamics was performed using elastic and quasielastic neutron scattering. In a neutron scattering experiment, neutrons are scattered by the atomic nuclei changing momentum and energy. The momentum transfer, $\hbar Q$, contains information about the spatial distance which is important for the scattering process, and the energy change, $\hbar\omega$, provides information about the time scale of motions in the sample. The outcome of the experiment is the scattering function $S(Q,\omega)$ that describes the probability of the momentum and energy transfer between neutron and sample. Thus, $S(Q,\omega)$ contains information about the sample structure and dynamics.

Several experiments have been undertaken to measure $S(Q,\omega)$ in a dynamical range as large as possible: (i) Time-of flight experiments measure the flight time between the scattering event and the detection at a scattering angle 2θ, the time-of flight data are then converted to $S(Q,\omega)$. The energy transfer is in the order of magnitude 0.1−250 meV that is typical of liquids. (ii) Backscattering experiments define and analyze the neutron energy with very high resolution using both monochromators and analyzer crystals at Bragg angle $\theta = 90°$ ($\delta E/E \sim \cot\theta\ d\theta$). The energy transfer is on the order of microelecronvolts, and the measured intensities are converted easily to $S(Q,\omega)$. With the time-of-flight instrument we measured the dynamics of water and in the backscattering spectrometers we measured the polymer dynamics. We have used two backscattering spectrometers to improve data fitting.

The experiments were carried out at the Institute Laue Langevin (ILL) in Grenoble, France, using the cold neutron backscattering spectrometers IN10 and IN16, and the time-of-flight spectrometer IN5.[20] When measuring on IN10, the analyzed neutron wavelength was kept always fixed at 6.271 Å using Si(111) crystals, while the incident neutron wavelength was set using two different monochromators. For "fixed energy window" scans centered at zero energy transfer (elastic scans) the incident wavelength was equally set to 6.271 Å by an equivalent Si(111) crystal. Thereby, an energy resolution of 1 μeV fwhm was obtained. The quasielastic measurements were performed by varying the lattice spacing of a KCl(200) monochromator crystal through controlled heating and cooling[20,21] and adjusted to cover an experimental energy transfer range of $-6\ \mu\text{eV} < E < +16\ \mu\text{eV}$. With this setup, an energy resolution of about 2 μeV fwhm was achieved. Measurements were carried out at seven scattering vectors covering the Q range between 0.5 and 2 Å^{-1} where Q is the momentum transfer defined by $Q = 4\pi \sin\theta/\lambda$, being 2θ the scattering angle. To better define the dependence of the quasielastic width with the scattering vector in the swollen state we have used the high flux spectrometer IN16 ($\Delta E \sim 1\ \mu$eV) in which measurements can be performed at 20 detectors covering approximately the same Q range as in IN10. The dynamics of the water was investigated using the time-of-flight spectrometer IN5 which covers an energy transfer range of $-2\ \text{meV} < E < +2\ \text{meV}$ with resolution ~100 μeV at 5.0 Å incident wavelength and 8500 rpm chopper speed.

Quasielastic spectra were recorded at 290 and 327 K for every Q. The geometry of the sample holder was double wall hollow cylinder which was sealed to avoid D_2O evaporation during the measurements. The thickness and concentration of the sample was selected to yield a transmission of about 85%. Standard ILL procedures and programs were used for corrections (empty cell), normalization and quasielastic peak fit.

Diffusion ordered spectroscopy (DOSY) was applied to separate the diffusion coefficients of water and PNIPAM. ^{1}H solution-state NMR measurements were preformed using pulsed field gradient (PFG−NMR) technique on a Bruker AVANCE AV-500 MHz instrument.[22] ^{1}H NMR were collected using 1.25−2.5 ms sine shaped gradient pulses ranging from 0.0067 to 0.3203 Tm^{-1} in 16 to 32 square spaced increments, with sample temperature of 298 K. Diffusion times were between 60 ms and 1 s. The gradient length and diffusion time were adjusted to achieve ~95% signal suppression at maximum gradient strength. PFG−NMR can only measure diffusion constant of polymers in solution. In our case, the attenuation of the PFG−NMR intensity was measured only in the swollen state of the microgel since in the collapsed state no signal was detected.

The volume phase transition of the particles was monitored by measuring its colloidal size with dynamic light scattering (DLS). We employed a Malvern Instruments 4700 experimental device equipped with a 5 mW helium−neon laser ($\lambda = 632.8$ nm) set to a scattering angle of 40°. The temperature was controlled to a precision of ±0.1 °C using a Peltier temperature-control system, aided by external water circulation. The mean diffusion coefficient was derived from the intensity autocorrelation function using cumulant analysis and converted into mean particle size via the Stokes−Einstein equation.

Electrophoretic mobility measurements were performed for sample control with a Malvern Zetasizer-Z, based on the principles of laser Doppler electrophoresis, equipped with a Peltier thermocouple (precision of ±0.1 °C). The cell temperature was determined with an external calibration to ensure precise temperature measurements. The dispersions are sufficiently dilute to ensure simple scattering. Since the probability for multiple scattering events increases with the particle−solvent refractive index difference, we perform intensity−concentration experiments for deswollen particles and select the solid content from the linear region to be $c \approx 0.02$ wt %.

Theory. Dynamics in polymeric systems result from the superposition of vibrations, rotations, and translational motions.[23–25] However, these motions are difficult to isolate, identify and properly characterize, even in chemically simple polymers, due to their different time and length scales. One way to extract information consists in differentiate between faster motions (vibration-like) and slower motions (diffusion-like). The time scales of these motions are sufficiently distinct from each other and, if the motions are uncoupled, features characteristic of different motions appear in separate regions of energy transfer (ω) in IQNS spectra. Furthermore, any rotational motion is generally very fast on the time scale of translational motions forming a low intensity flat background that can be separated when using high resolution spectrometers like IN10 or IN16.

The diffusive translational motion of the polymer chain in water is retarded because the drag friction between the network and water. The equation for the displacement **r** of a point in the microgel whose average location was x obeys the linear equation[16]

$$\rho(\partial^2/\partial t^2)\vec{r} = K(\partial^2/\partial x^2)\vec{r} - f(\partial/\partial t)\vec{r} \quad (1)$$

The left-hand side represents the density ρ times the acceleration. The first term in the rhs is the elastic restoring force (with elastic modulus K) and the second term is the friction between the network and the water. In microgels the inertia term is smaller than the friction and elastic terms allowing us to write

$$(\partial/\partial t)\vec{r} = (K/f)(\partial^2/\partial x^2)\vec{r} \quad (2)$$

The polymer undergoes a diffusive-like motion[22] which is characterized by a diffusion coefficient $D = K/f$. Taking into account the above considerations, the analysis of the IQNS data was done considering the molecular motion formed by the combination of a faster motion characterized by the mean square displacement $\langle u \rangle$, given by the Debye−Waller factor, and a translational diffusion motion characterized by the diffusion coefficient D. For Fickian diffusion the dynamic structure factor is a Lorentzian function, with half-width at half-maximum DQ^2. Assuming that the faster and the diffussional motions are uncoupled, the incoherent scattering function can be written

$$S(Q,\omega) = \exp(-\langle u^2 \rangle Q^2/3)\delta\omega \otimes \frac{1}{\pi}\frac{DQ^2}{(DQ^2)^2 + \omega^2} \qquad (3)$$

where $\otimes$ is the convolution product in ω. The mean square displacement $\langle u^2 \rangle^{1/2}$ can be obtained analyzing the Q dependence of $S(Q,0)$ at fixed temperature, and D can be derived from the fitting of the quasielastic component of the IQNS patterns.

Results

Figure 1 shows a SEM micrograph of dry PNIPAM microgels. The microgels present a well defined spherical shape with low size dispersion.

We use DLS to follow the volume phase transition of the PNIPAM microgels with increasing temperature. The dispersions were sufficiently dilute to ensure simple scattering. Since the probability for multiple scattering events increases with the particle-solvent refractive index difference, we perform intensity−concentration experiments for deswollen particles and select the solid content from the linear region to be $c \approx 0.02$ wt %. This concentration also guaranties absence of interactions between particles, as confirmed by measuring the electrophoretic mobility versus particle concentration which is constant as shown in the inset of Figure 1. The particles shrink continuously with increasing T; this occurs due to the temperature dependence of the Flory χ parameter controlling the polymer solvency in the surrounding medium. The maximum slope of the size-temperature curve is located at $T_t = (31.9 \pm 0.2)$ °C, in agreement with previous results. We note the high swelling ratio of our system, $D(T_{swollen})/D(T_{deswollen}) \approx 4$, resulting from the low polymer mesh cross-linking employed in the synthesis; this allows higher swelling ratios with respect to those typically reported for PNIPAM particles. Furthermore, the swelling process is thermo-reversible which is characteristic for chemical cross-linked polymer networks.

From neutron scattering measurements we obtain the double differential scattering cross section $d^2\sigma/(d\Omega\ dE)$, which is proportional to the coherent $S_{coh}(Q,\omega)$ and the incoherent $S_{inc}(Q,\omega)$ scattering functions. The incoherent scattering cross section of hydrogen is very large in comparison with the coherent and incoherent scattering cross sections of other atoms in the sample such as carbon, oxygen and nitrogen. For pure PNIPAM the ratio $\sigma_{inc}(H)/\sigma_{inc}(polymer)$ is 0.9997. Accordingly, from the measurements we obtain $S_{inc}(Q,\omega)$ for the H atoms and hence, we can infer the dynamics of the polymeric chain to which the H atoms are attached. Nevertheless when the objects of study are microgel dispersions in D_2O, the incoherent and coherent scattering signal of the solvent must be separated from those arising from the sample. In principle, the backscattering or time-of-flight instruments do not allow discrimination between coherent and incoherent scattering and, thus, measurements contain both contributions. However, the bulk liquid-water coherent-scattering predominantly appears concentrated at the intermolecular O−H peaks[23] at ca. 1.8 and 3.3 Å^{-1}. On the other hand, the first crystalline peak of ice, the (110) reflection, appears at $Q \cong 1.597$ Å^{-1} and the region below this Q value is featureless.[24] Taking this into account, it was possible to get rid of most of the water coherent scattering performing the experiments placing the detectors at Q values below 1.5 Å^{-1} where no water structure is observed and the coherent contribution is very small. On the other hand, the IQNS data obtained from the few detectors left at Q higher than 1.5 Å^{-1} follow nicely the trend marked by the detectors at lower Q, which seems to indicate a small coherent contribution in that region too. However, the data are presented as $S(Q,\omega)$ instead of $S_{inc}(Q,\omega)$ because some coherent scattering can contribute at the higher Q values.

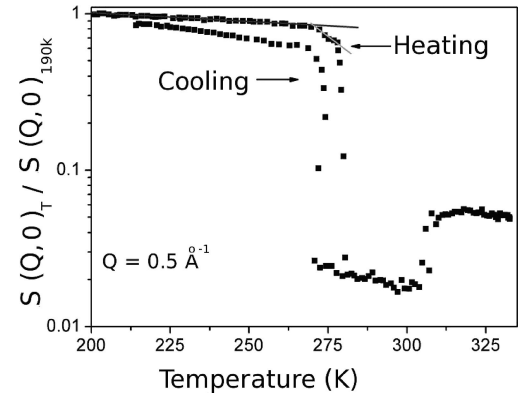

Figure 2. Normalized elastic scattering function from IN10 spectrometer ($Q = 0.5$ Å^{-1}), plotted in logarithm scale, for the heating and cooling cycle of 0.25 wt % cross-linked PNIPAM microgels. The heating rate was 0.4 K/min.

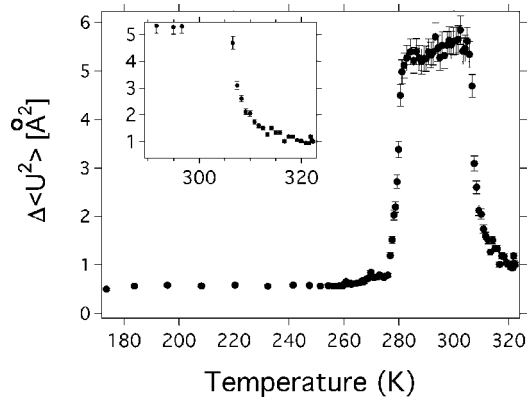

Figure 3. Oscillations of the vibrational amplitude of the network showing different behavior depending on the dispersion temperature.

Inelastic neutron scattering was employed to extract space- and time-dependent information about the microscopic dynamics.[25−27] The elastic neutron-scattering function $S(Q,0)$ was measured as a function of temperature with IN10 using the so-called "fixed elastic window" method.[25] The elastic scans provide an overview about the temperature dependence of the molecular dynamics.

Figure 2 shows $S(Q,0)$ measurements normalized to its value at 190 K ($S(Q,0)_{190K}$), well below the freezing temperature of deuterated water, plotted on a logarithmic scale during a heating and cooling cycle. The intensity linearly decreases with increasing temperature up to 273 K.

Between 273 and 277 K, the intensity continues its linear decrease but with a higher slope until 277 K where a pronounced decrease is observed corresponding to the melting of D_2O. The steep decrease is attributed to the motions induced on D_2O molecules at the melting temperature that broadens the elastic component with the corresponding shift outside the "fixed energy window" and the subsequent drop of the elastic intensity. The opposite trend is observed in Figure 3 at 306 K, corresponding to the microgel volume phase transition temperature where the intensity exhibits an steep increase during the heating process. In most phase transitions, as it occurred at the melting of D_2O, $S(Q,0)$ decreases at the transition temperature which indicates the onset of some molecular motions. On the contrary, the increase of $S(Q,0)$ observed at the volume transition indicates that some polymer motions activated below the transition temperature are hindered when the microgel collapses. For the cooling process, the opposite behavior is observed at both transitions respectively.

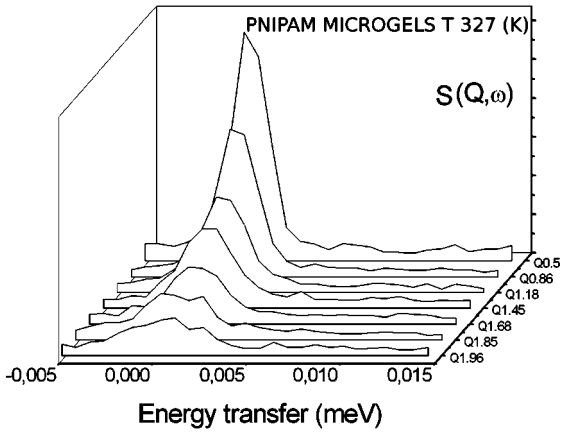

Figure 4. Quasielastic neutron scattering spectra as a function of Q for 0.25% cross-linked PNIPAM microgels at 327 K.

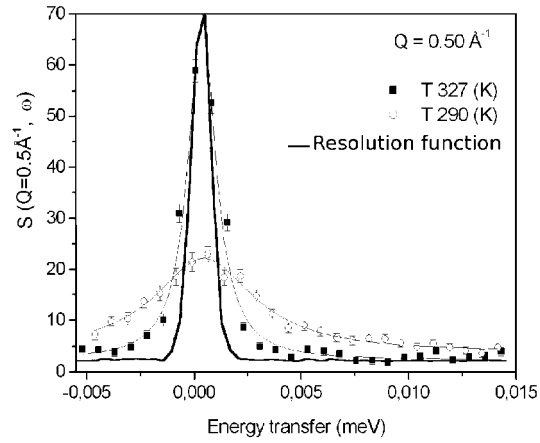

Figure 5. The $S(Q,\omega)$ function clearly shows the different dynamics of the 0.25 wt % cross-linked PNIPAM network in the swollen (290 K) and collapsed (327 K) states. The solid lines through the points represent the fitting results with equation 3. The solid continuous line corresponds to the resolution function.

The spatial scale of the vibrational motion of the scattering particles (mostly hydrogen), the root of the mean square displacement $\langle u^2\rangle^{1/2}$, can be obtained analyzing the Q dependence of $S_{inc}(Q,0)$ at fixed temperature

$$\ln\frac{S_{inc}(Q,0)}{S_{inc}(Q,0)^{190K}} = -\frac{1}{3}[\langle u^2(T)\rangle - \langle u^2(190K)\rangle]Q^2 \qquad (4)$$

The temperature dependence of $\Delta\langle u^2\rangle = \langle u^2(T)\rangle - \langle u^2(190\ \text{K})\rangle$ is shown in Figure 3.

Figure 3 reveals that in the temperature range from 190 up to 260 K $\Delta\langle u^2\rangle$ remains nearly constant since the solvent is frozen and the faster motions are absent. Nevertheless at 260 K we observe an increase in $\Delta\langle u^2\rangle$, which reaches a steep increase at 278 K related with the gain of freedom of molecular motions after the melting of the solvent. Such increment in $\Delta\langle u^2\rangle$ reaches a maximum of 5 Å^2 at 282 K. From 282 to 306 K, increments in the temperature provoke an increase in the $\Delta\langle u^2\rangle$, which is a normal "Debye−Waller" behavior. However, when the temperature is around 306 (above the LCST of the PNIPAM), the linear behavior of $\Delta\langle u^2\rangle$ vs T disappears; the amplitude exhibits a steep decrease reaching similar levels to the frozen network. This fact indicates that in the collapsed state the faster motions of the polymeric chain are hampered and the system behaves like-solid material.

We have investigated with IN10 the IQNS at 290 and 327 K, below and above the volume transition temperature respectively. At 290 K the quasielastic signal appeared only at the two detectors placed at low Q. For $Q > 0.86$ Å^{-1} the signal could not be measured due to the increase of the noise/signal ratio. On the contrary, as is shown in Figure 4, at 327 K the intensity is much greater and was measured over the seven detectors of the IN10 spectrometer.

In Figure 5, we show the quasielastic component for $Q = 0.5$ Å^{-1} at the two selected temperatures together with the fitting result obtained using the expression given by eq 3 and the resolution function. Experimental data are represented by points and the result of the fitting by continuous lines. The result of the fitting was improved by introducing a flat background whose value is determined from the data of the tails of the curve. The flat background indicates that other motions in the millielectronvolt region such as water or polymer rotational motions are activated.

As was stated before, a possible contribution to the polymer incoherent scattering signal could arise from the water incoherent scattering. In our experiments the σ_{inc}(NIPA)/σ_{inc}(total) is 0.54 and the rest of the incoherent signal comes from D_2O. Nevertheless, the D_2O dynamics is about 2 orders of magnitude faster than the polymer dynamics. To prove that the dynamics

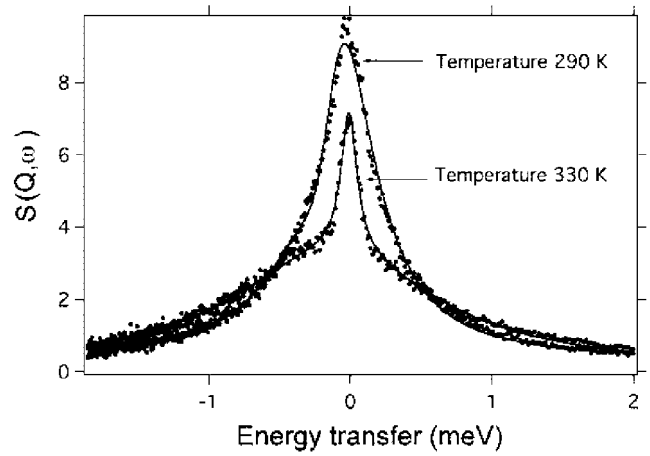

Figure 6. Quasielastic neutron scattering spectra recorded in IN5 at $Q = 0.45$ for 0.25 wt % cross-linked PNIPAM microgels at 290 and 330 K.

of D_2O can be experimentally distinguished from the polymer dynamics we have performed measurements in IN5. The energy range of IN5 permits to observe the contribution of water and polymer to the incoherent scattering and because the different timescales of solvent and main polymer dynamics the solvent contribution can be removed. This assumption was confirmed by the measurements of the 0.25 wt % cross-linked PNIPAM microgels solution at 290 and 330 K performed in IN5. As can be seen in Figure 6, at 290 K water gives a quasielastic contribution in the energy range of the meV that broadens as the temperature increases up to 330 K. In Figure 6, one can observe that the scattering of the sample is the result of two components, the dynamics of the water molecules and the polymer dynamics. At 330 K, the microgel is in the collapsed state producing a narrowing in the polymer scattering contribution around the elastic peak compared with those obtained at 290 K whereas the D_2O contribution widens due to the increment in the mobility of the water molecules.

The main conclusion of the study in IN5 is to show that the contribution of the solvent to the incoherent scattering appears as a constant background at the ± 15 μeV window of IN10 and IN16 spectrometers.

From the fitting with a Lorentzian function in Figure 5, we obtained the half-width at half-maximum $\Gamma(Q)$. To better define the Q dependence of the IQNS signal in the swollen state we

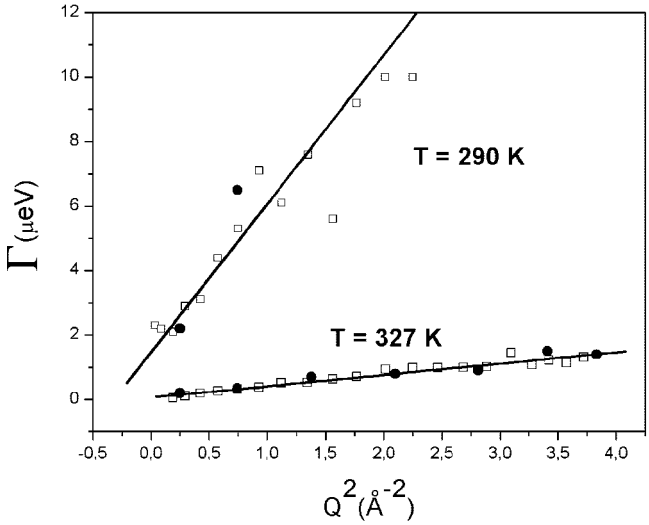

Figure 7. Half-width at half-maximum of the Lorentzian quasielastic component measured in IN10 (black circles) and in IN16 (white squares) spectrometers as a function of Q^2 for the microgels in the swollen (290 K) and collapsed (327 K) states.

Table 1. PNIPAM (0.25% Cross-Linked) Experimental Diffusion Constant Calculated from IQNS and PFG−NMR Measurements

PNIPAM 0.25 wt % cross-linking	IQNS	PFG−NMR
D (swelled) (10^{-11} m^2/s) $T = 290$ K	1.1 ± 0.2	4.09 ± 0.05 0.47 ± 0.05
D (collapsed) (10^{-13} m^2/s) $T = 327$ K	8.6 ± 0.1	

have repeated the measurement in the high flux spectrometer IN16. In Figure 7, we represent together the values of Γ versus Q^2 obtained at 327K and at 290K in both spectrometers; IN10 and IN16.

The relaxation time of the polymer network can be expressed $\Gamma = DQ^2$. In the swollen state we obtained $D = 1.9 \pm 1.0 \times 10^{-11}$ m^2/s using the data from IN10 and $D = 1.1 \pm 0.2 \times 10^{-11}$ m^2/s using the data from IN16 whereas in the collapsed state we obtained the same value, $D = 8.6 \pm 0.1 \times 10^{-13}$ m^2/s, with both spectrometers. In the swollen state, we have selected the D value obtained with IN16 due to the large uncertainty of the value derived from IN10 because the lack of experimental points. The polymer diffusion coefficients are summarized in Table 1. The variation of D follows an opposite tendency to most solids and liquids for which D increases when temperature is raised. The values of the diffusion coefficient are of the same order of magnitude as those measured in PNIPAM macrogels using different techniques.[18]

As we have pointed out before, the microgel solutions are dilute and the incoherent cross section of PNIPAM is similar to that of the HDO. Diffusion ordered NMR spectroscopy (DOSY) permits to read separately the diffusion coefficients of the polymer and HDO. Figure 8B shows the diffusion peaks of the different ^{1}H in the polymer chain positioned between 0.6 and 5.0 chemical shift in ppm with log D around −11. On the contrary, the diffusion peak for the HDO molecule is well resolved and appears separated from these peaks and positioned at 4.75 ppm with log D around −8.8. The assignment of the ^{1}H lines of backbone and side-chain protons refer to the monomer scheme given in Figure 8A. The proton on the amino group can not be identified due to the fast exchange with the water deuterons, so that the signal is buried in the HDO resonance.[28]

We have selected the ^{1}H of the methyl group at 0.95 ppm to perform PFG −NMR spectroscopy for an accurate determination

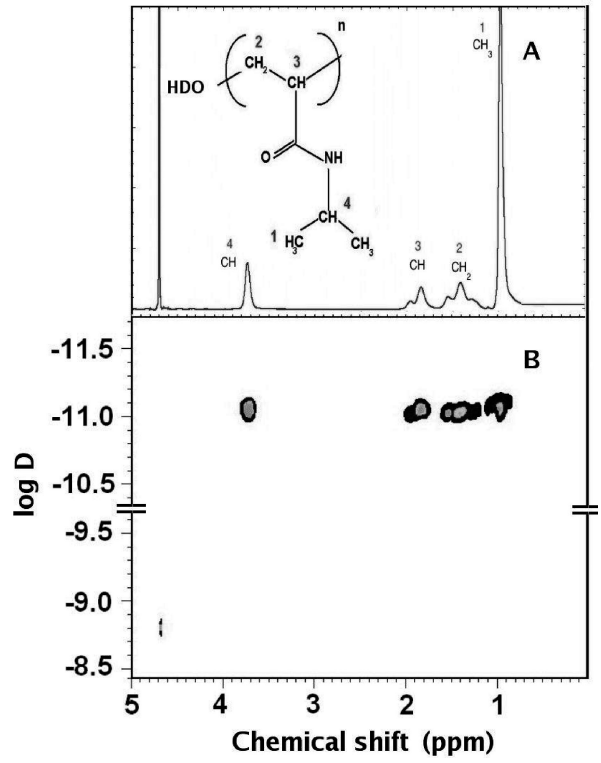

Figure 8. (A) ^{1}H DOSY scan spectra and the chemical structure of NIPAM. The assignment of the ^{1}H lines refers to the monomer scheme given in the figure. (B) DOSY display of the PNIPAM microgels (calculated with CONTIN) in the swollen state (290 K).

of the diffusion constant. There are many papers on diffusion of polymer gels by PFG−NMR.[29–32] By use of a gradient, molecules can be spatially labeled, i.e., marked depending on their position in the sample tube, and if they move during a certain time (the diffusion time, Δ) a second gradient is used to decode their new position. The intensity attenuation of the NMR signal depends on the gradient parameters (g, δ, τ) and the diffusion time Δ

$$\ln\left(\frac{I}{I_0}\right) = -D\gamma^2 g^2 \delta^2 (\Delta - \delta/3 - \tau/2) \quad (5)$$

where I is the observed intensity, I_0 is the intensity in the absence of gradient pulses, D the diffusion coefficient, γ the gyromagnetic ratio of the observed nucleus, g the gradient strength, δ the length of the gradient, and τ the time between bipolar gradients.[33] The plot of $\ln[I/I_0]$ against $(\gamma g \delta)^2 (\Delta - \delta/3 - \tau/2)$ gives a straight line with a slope of $-D$ if the diffusion of probe molecules is in a single diffusion component.

Initially, to calibrate the equipment, the self-diffusion coefficient of HDO in D_2O was measured at 17 and at 54 °C and compared with literature values. Figure 9 shows the plot of $\ln[I/I_0]$ against $(\gamma g \delta)^2 (\Delta - \delta/3 - \tau/2)$.

It is seen from these plots that the experimental data lie on a straight line. At 17 °C a value of $D = 2.03 \pm 0.05 \times 10^{-9}$ m^2 s^{-1} was obtained that agrees well with the value previously reported.[34] At 54 °C, a value of $3.62 \pm 0.05 \times 10^{-9}$ m^{2}s^{-1} was obtained.

For microgels, it is well-known that a fraction of the water is bound to specific sites within the polymer network and as a consequence the diffusion coefficient of HDO should decrease.[35] The diffusion coefficient of HDO in a dispersion of PNIPAM microgels in D_2O (3 wt %) was measured at 17 °C and a value of $1.78 \pm 0.05 \times 10^{-9}$ m^2 s^{-1} was obtained. The observed reduction of the HDO diffusion coefficient is a direct confirmation of the influence of bound water in the experimental value

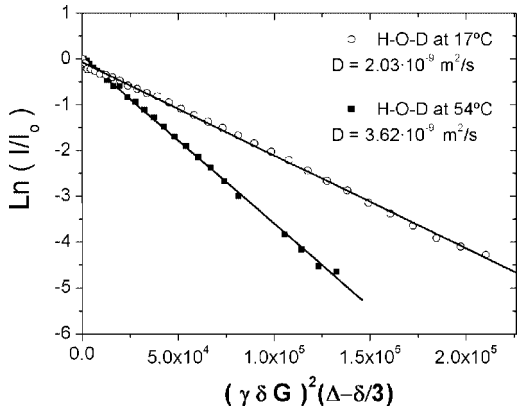

Figure 9. ^{1}H PFG−NMR of HOD in D_2O used for calibration. ^{1}H NMR were collected using 1.25−2.5 ms sine shaped gradient pulses ranging from 0.0067 to 0.3203 Tm^{1-} in 16 to 32 square spaced increments. Diffusion times were between 60 ms and 1s. A typical Stejskal-Tanner plot of the experimental peak areas at 17 °C (○) and at 54 °C (■). The solid lines represent linear least-squares fits to the data.

Table 2. Water Diffusion Coefficients Calculated from PFG−NMR Measurements in Pure Water and in an Aqueous Dispersion of PNIPAM (3 wt %)

PFG−NMR measurements	HDO in D_2O	HDO in dispersion of PNIPAM in D_2O
D (10^{-9} m^2/s) T = 290 K	2.03 ± 0.05	1.78 ± 0.05
D (10^{-9} m^2/s) T = 327 K	3.62 ±0.05	

of the diffusion coefficient (see Table 2). The HDO−NIPAM interactions impose a restriction on the mobility of the HDO molecules, decreasing the HDO diffusion coefficient in the microgel dispersion.

The plot of I/I_0 (in logarithmic scale) for PNIPAM microgels in the swollen state against $(\gamma g\delta)^2$ $(\Delta - \delta/3 - \tau/2)$ consists of two straight lines with different slope as shown in Figure 10.

This means that the polymer diffusion has two components: a slow diffusion component and a fast diffusion component. The diffusion coefficients for both components, determined from the slopes are on the order of 10^{-11} m^2/s and are given in the second column of Table 1.

The slow diffusion component may be assigned to the microgel regions with higher cross-linker content, predominantly placed in the particle core, where the polymer chain suffers the partial-restriction effect imposed by the cross-linkers. On the contrary, the fast diffusion component would be associated with regions with lower cross-linking content, where the diffusive motion of the polymer chain is less restricted. In this scenario, the diffusion coefficient, calculated from IQNS, represent an average value because neutrons can not differentiate H nucleus placed in both portions of the microgel.

Conclusions

The dynamics of the polymer chains in a PNIPAM microgel has been studied by IQNS and PFG−NMR. From IQNS measurements two motions were identified: (i) a faster motion of Debye−Waller type which shows up as a sharp steep in *S(Q,0)*) at the volume phase transition; (ii) a diffusive-like motion with a diffusion coefficient that decreases when the temperature increase and the microgel collapses. Moreover, two diffusion components in the swollen microgels were identified. It can be said that the slow and fast diffusion components can be assigned to microgel regions with high and low cross-linking contents respectively. In the core of the microgel, patches with high cross-linking content would be predominant forming the microgel core observed by SANS. Thus, the slow and fast diffusion coefficients measured with PFG−NMR would be the dynamic counterparts of the core−shell structure observed by SANS.

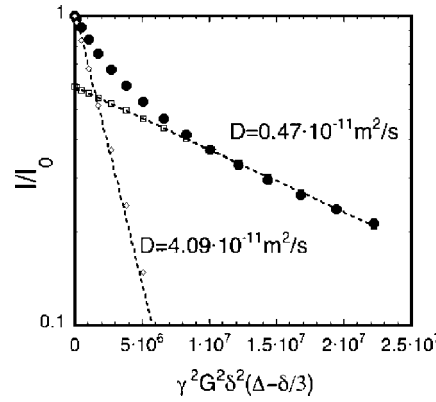

Figure 10. Plot of I/I_0 against $(\gamma g\delta)^2$ $(\Delta - \delta/3 - \tau/2)$ for PNIPAM 0.25% microgels at 290 K in the swollen state.

Acknowledgment. This work was supported by Ministry of Science and Technology (MAT2006-13646-C03-01 and MAT2006-13646-C03-02), from the CAM-UCM Program to support research groups (CCG07-UCM/MAT2480), the COST Action D43, and Junta de Andalucía (FQM-02353). J.R.R. acknowledges the Areces Foundation for a postdoctoral fellowship to perform this work.

References and Notes

(1) Pelton, R. *Adv. Colloid Interface Sci.* **2000**, *85*, 1.
(2) Fernandez-Nieves, A.; Fernandez-Barbero, A.; de las Nieves, F. J.; Vincent, B. *J. Phys.: Condens. Matter* **2000**, *12*, 3605.
(3) Fernandez-Nieves, A.; Fernandez-Barbero, A.; de las Nieves, F. J. *Langmuir* **2000**, *16*, 4090.
(4) Hirotsu, S.; Hirokawa, Y.; Tanaka, T. *J. Chem. Phys.* **1987**, *87*, 1392.
(5) Yong, L.; Tanaka, T. *J. Chem. Phys.* **1987**, *90*, 5161.
(6) Jun, L.; Xia, H.; Yang, L. Y.; Di, L.; Yongwei, W.; Jinghong, L.; Yubai, B.; Tiejin, L. *Adv. Mater.* **2005**, *17*, 163.
(7) Takeoka, Y.; Watanabe, M. *Adv. Mater.* **2003**, *15*, 199.
(8) Lee, Y. J.; Braun, P. V. *Adv. Mater.* **2003**, *15*, 563.
(9) Zhibing, H.; Xiaohu, X. *Adv. Mater.* **2004**, *16*, 305.
(10) Pelton, R. *Adv. Colloid Interface Sci.* **2000**, *85*, 1.
(11) Fernandez-Nieves, A.; Fernandez_Barbero, A.; De las Nieves, F. *J. Chem. Phys.* **2001**, *115*, 1.
(12) Fernandez-Barbero, A.; Fernandez-Nieves, A.; Grillo, I.; López Cabarcos, E. *Phys. Rev. E* **2002**, *66*, 051803.
(13) Saunders, B. A. *Langmuir* **2004**, *20*, 3925.
(14) Berndt, I.; Pedersen, J. S.; Richtering, W. *J. Am. Chem. Soc.* **2005**, *127*, 9372.
(15) Stieger, M.; Richtering, W.; Pedersen, J. S.; Lindner, P. J. *Chem. Phys.* **2004**, *120*, 6197.
(16) Tanaka, T.; Lon, O. H.; Benedek, G: B. *J. Chem. Phys.* **1973**, *59*, 5151.
(17) Shibayama, M.; Shirotani, Y.; Shiva, Y. *J. Chem. Phys.* **2000**, *112*, 442.
(18) Takahashi, K.; Takigawa, T.; Masuda, T. *J. Chem. Phys.* **2004**, *120*, 2972.
(19) Pelton, R. H.; Chibante, P. *Colloids Surf.* **1986**, *247*, 20.
(20) The instrument user′s guide can be found athttp://wwwold.ill.fr/index_sc.html.
(21) Cook, J. C.; Petry, W.; Heidemann, A.; Barthélemy, J. F. *Nucl. Instrum. Methods Phys. Res., Sect. A* **1992**, *312*, 553.
(22) Stejskal, O. E.; Tanner, E. J. *J. Chem. Phys.* **1965**, *42*, 288.
(23) Petkov, V.; Peng, Y.; Willians, G.; Huang, B.; Tomalia, D.; Ren, Y. *Phys. Rev. B* **2005**, *72*, 195402.
(24) Wollan, E. O.; Davidson, L.; Shull, C. G. *Phys. Rev.* **1949**, *75* (9), 1348.
(25) Bee, M. In *Quasielastic Neutron Scattering*; Adam Hilger (IOP): Bristol, U.K., 1988.
(26) Lopez Cabarcos, E.; Batallan, F.; Frick, B.; Ezquerra, T.; Balta Calleja, F. J. *Phys. Rev. B* **1994**, *50*, 13214.

(27) Ryong-Joon, R. In *Methods of X-Ray and Neutron Scattering in Polymer Science*; Oxford University Press, Inc.: New York, 2000.
(28) Larsson, A.; Kuckling, D.; Schönhoff, M. *Colloid Surf. A: Phys. Chem. Eng. Asp.* **2001**, *190*, 185.
(29) Matsukawa, S.; Ando, I. *Macromolecules* **1996**, *29*, 7136.
(30) Masaro, L.; Zhu, X. X.; Macdonald, P. M. *Macromolecules* **1998**, *31*, 3880.
(31) Yamane, Y.; Matsui, M.; Kimura, H.; Kuroki, S.; Ando, I. *Macromolecules* **2003**, *36*, 5655.
(32) Kamiguchi, K.; Kuroki, S.; Satoh, M.; Ando, I. *Polymer* **2005**, *46*, 11479.
(33) Johson, C. S. *Prog. Nucl. Magn. Reson. Spectrosc.* **1999**, *34*, 203.
(34) Danielsson, J.; Jarvet, J.; Damberg, P.; Gräslund, A. *Magn. Reson. Chem.* **2002**, *40*, 589.
(35) Sierra-Martin, B.; Choi, Y.; Romero Cano, M. S.; Cosgrove, T.; Vincent, B.; Fernandez-Barbero, A. *Macromolecules* **2005**, *38*, 10782.

MA800668T